STRENGTH PROPERTIES AND FRACTURE TOUGHNESS OF HIGH STRENGTH HARDOX-400 STEEL IN BRITTLE-TO-DUCTILE TEMPERATURE INTERVAL

FURMAŃCZYK Piotr[1], PAŁA Robert[2], DZIOBA Ihor[2]

[1]Kielce University of Technology, Faculty of Mechatronics and Machine Design, Department of Applied Computer Science and Armament Engineering, Kielce, Poland, EU
[2]Kielce University of Technology, Faculty of Mechatronics and Machine Design, Department of Machine Design Fundamentals, Kielce, Poland, EU

Abstract

The paper presents experimental results concerning changes in strength and fracture toughness characteristics of Hardox-400 high-strength steel in brittle-to-ductile temperature range from -100 °C to +20 °C. It was shown that the values of strength properties increased linearly with the lowering of the temperature during the test. The changes in fracture toughness characteristics with temperature are more complex and they will be described by the exponential type function.

Keywords: Hardox-400 high-strength steel, strength properties, fracture toughness

1. INTRODUCTION

Over the last decade, the application range of high-strength ferritic steels, namely S960QC, Hardox, Weldox has been extended. The steels are used in different structures that often operate are under low temperature conditions. In addition to high values of strength properties, those steels often have high plasticity. As a result, they show high fracture toughness and a low temperature of transition to brittle fracture. The knowledge of the levels of steel properties in the temperature service range is necessary to make a correct assessment of steel strength, and to ensure failure-free operation. This study presents the results of investigations which made it possible to establish how the changes in Hardox-400 steel strength characteristics and fracture toughness depend on temperature in the temperature range corresponding to ductile-to-brittle transition.

Table 1 Chemical composition of Hardox-400 steel according to manufacturer [3]

C, %	Si, %	Mn, %	P, %	S, %	Cr, %	Ni, %	Mo, %	B, %
0.18	0.70	1.60	0.025	0.010	1.00	0.25	0.25	0.004

2. TEST MATERIAL

Tests were conducted on specimens of Hardox-400 steel, the chemical composition of which is shown in **Table1**. The specimens had the form of 30 mm thick plates. Due to the character of thermomechanical treatment carried out by the manufacturer, 30 mm thick plates demonstrate a reduction in hardness from 400 HV on the surface by approx. HV 50 HV, over the thickness, in the central zone, which was reported in study [1]. To eliminate the influence of microstructure changes on the level of the material characteristics, the tested specimens were cut out from the central part of the plate thickness. Hardox-400 steels exhibit tempered martensite structure, with small particles of carbides precipitated along grain boundary, and large particles of titanium nitrides enriched with Nb, which was confirmed by EDS analysis of oxides and sulphides [2].Chemical composition shows **Table 1**.

3. DETERMINATION OF STRENGTH PROPERTIES AND FRACTURE TOUGHNESS

Strength properties were determined in the uniaxial tensile test using cylindrical specimens, 5 mm in diameter [1]. As can be seen in the **Figure 1**, determined strength properties, yield strength - σ_y, ultimate tensile strength - σ_{ut}, Young's modulus - E, material hardening coefficient - n show scatter, which is caused by inhomogeneity of the material. The values of mechanical characteristics obtained at different temperatures were described with linear functions. Such an approach was proposed by the authors in earlier studies [1]. In this paper, the datasets used to establish the dependences between mechanical characteristics and temperature were extended. Functional dependences make it possible to obtain averaged values of characteristics, because they are compiled on the basis of the data from tests on many specimens.

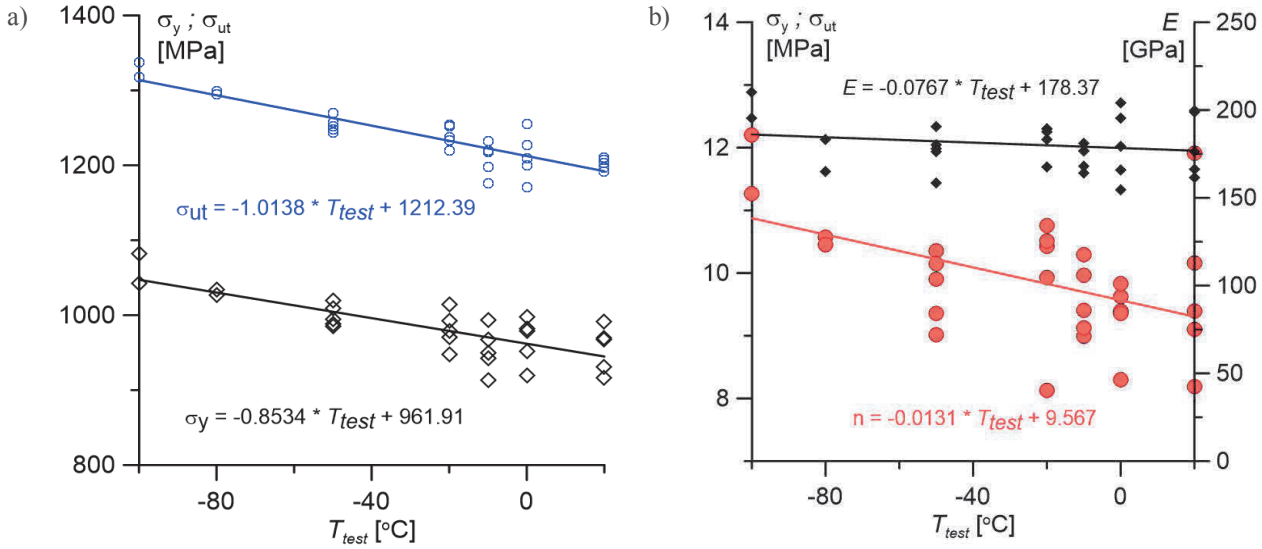

Figure 1 Influence of temperature on strength characteristics a) yield strength, ultimate tensile strength, b) material hardening coefficient, Young's modulus

Tests of fracture toughness were conducted on standard single edge notch bending specimens SEN(B), which had a thickness of B = 12 mm and a width of W = 24 mm. Fatigue cracks were generated from the bottom of the chevron notch that was mechanically cut using a controlled force. The length of the fatigue crack ranged $0.45 < a_0 / W < 0.65$. Thus, the requirements posed by ASTM standard for SEN(B) specimens preparation for by fracture toughness tests were satisfied [4]. The tests at below-zero temperatures were conducted in the thermal chamber in the nitrogen vapour medium. To determine the actual crack length in loading, the potential drop technique was used [5]. Signals of force, specimen deflection and potential difference that were recorded made it possible to plot the curve J_R, and to determine a critical value of integral J, J_C in the case of crack growth in accordance with the ductile fracture mechanism. In the case of brittle fracture occurrence, without ductile growth, fracture toughness is determined from formula $J_C = 2A/(B - (W-a_0))$, where A is energy, determined as the area below the force-specimen deflection curve until the instant of brittle fracture start. The condition that specifies the specimen thickness which ensures the domination of the plane strain $B > B_C = 25 \cdot J_C / \sigma_y$ was satisfied for all tested specimens, hence $J_C = J_{IC}$ [4]. The highest values of fracture toughness were found at the temperature of +20 °C. As the temperature decreased, the values of the crack growth and levels of the critical values of fracture toughness decreased also. The scatter of data is caused by inhomogeneity of steel microstructure and the presence of brittle inclusion particles - sulphides, titanium nitrides, and oxides that initiate the fracture process. The procedure for determination of the critical value of integral J, J_{IC}, shown in ASTM standards, gives the critical value at the instant when the average length of subcritical crack is reached Δa = 0.2 mm. In the strength analysis of components with cracks, it is also

necessary to know the values of the integral J at the moment of the initiation of subcritical fracture, i.e. J_i. The procedure for the determination of the values of J_i is based on the determination of the stretch zone width (Δa_{SZW}), which occurs prior to subcritical crack initiation [6, 7, 8]. Some relations were proposed, which express the dependence between Δa_{SZW} and J_i [9, 10]. The investigations conducted by the authors showed that for ductile steels, the formula devised by Shih [10] is the most appropriate one.

$$J_i = (2\sigma_f / d_n)\Delta \overline{a}_{SZW} \tag{1}$$

where: $\sigma_f = 0.5(\sigma_y + \sigma_{ut})$; d_n - function dependent on the material hardening coefficient n and triaxiality coefficient $T_Z = \sigma_{33} / (\sigma_{11}+\sigma_{22})$, and also implicitly dependent on yield strength σ_y and Young's modulus E [10,11,12]; σ_{11}, σ_{22}, σ_{33} - stress components in the direction of crack growth, opening the crack plane and in the direction of the specimen thickness.

Coefficient d_n determined on the basis of formulas from study [11]:

$$d_n = d_0 - (2T_z)^{a_3(n)}(d_0 - d_5) \tag{2a}$$

for $n > 5$:

$$\begin{aligned} d_0 &= 1 - 0.1240(1/n)^{1/2} + 0.8968(1/n) - 13.3941(1/n)^{3/2} + 15.3139(1/n)^2; \\ d_5 &= 0.78 + 0.0277(1/n)^{1/2} - 3.0791(1/n) + 2.4709(1/n)^{3/2}; \\ a_3(n) &= 11.4 - 45.8(1/n) \end{aligned} \tag{2b}$$

Values T_z were computed based on stress distribution data, which were determined in numerical methods for the specimen longer axis plane. It is done so because the fracture process starts at this site, and the maximum level of opening stress σ_{22} occurs there (**Figure 2b**).

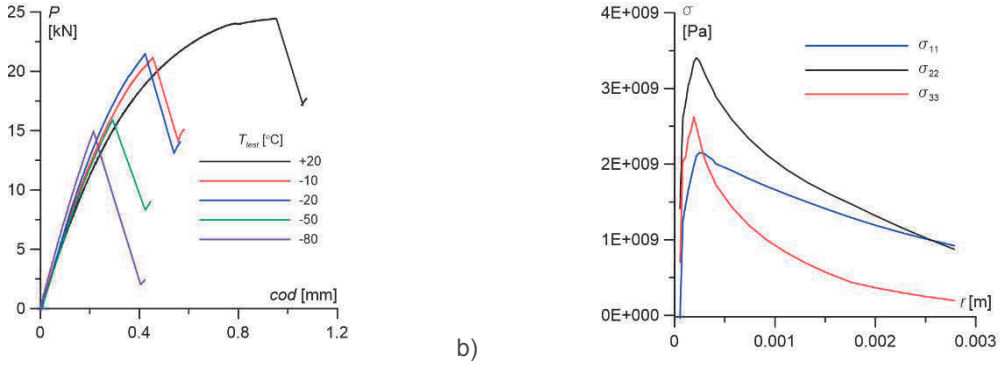

a) b)

Figure 2 a) curves of the loading force in the function of the crack opening displacement; b) distributions of stress components in front of a crack tip in the specimen axis for T_{test} = -10°C

When making numerical calculations, the process of SEN(B) specimen loading was simulated. The material was defined on the basis of true tension curves obtained, for individual temperatures, in uniaxial tensile tests. The crack tip was represented as a quarter of an arch with a radius of 10 μm. The loading was performed by shifting the loading roll to the site corresponding to the instant the critical value of the integral J, J_i, is reached. In calculations, the large strain model was assumed.

The standards that are available suggest that the computations of the value of the integral J, J_i, should be based on the determined stretch zone width [6, 7, 8]. On the fracture surface, this area is observed between the fatigue fracture zone and of the crack extension zone (**Figures 3a, 4**). The measurements of the SZW

were taken in compliance with European recommendations reported by ESIS [6] and GKKS [7], and with standard ISO-12135:2002 [8]. In accordance with the guidance provided by the standards, the measurements of the SZW were taken with *SEM JEOL* JSM-*7100F* with field emission. The measurement area was 1 mm in length, and it was located in the proximity of the fracture symmetry axis. The distance between the central points of measurement areas was 300 μm, and the fracture axis determinant was the crack initiator tip (**Figure 3b**). The value of Δa_{SZW} was obtained due to the measurement of the SZW from three measurement sites. In order to determine Δa_{SZW} from the SZW seen in SEM images, freely available open source IMAGE J software was used [13].

The determination of the SZW by means of estimation of the area offers much more accurate value than that from discrete measurements. That results from irregularities in stretch zone occurrence, and in some cases, from difficulties in finding the beginning and end of the zone (**Figure 4**).

a)

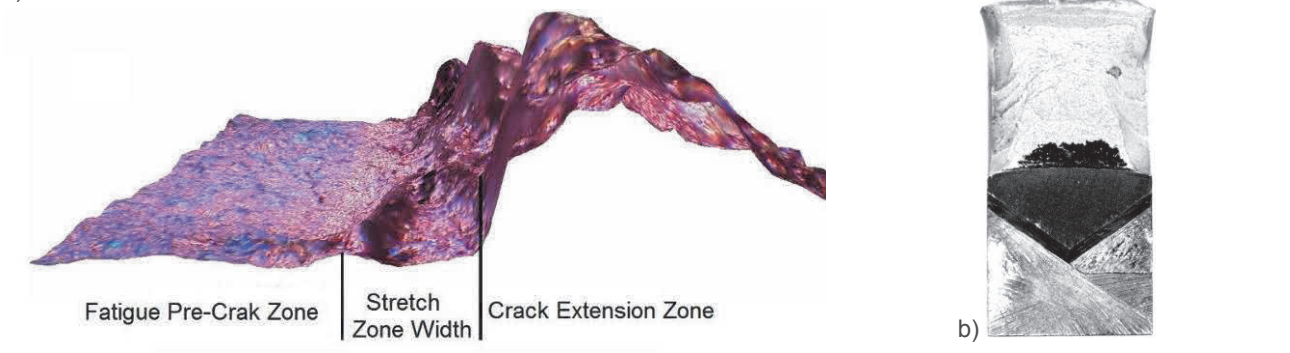

Figure 3 a) surface profile of the SEN(B) specimen breakthrough; b) view of specimen macro breakthrough

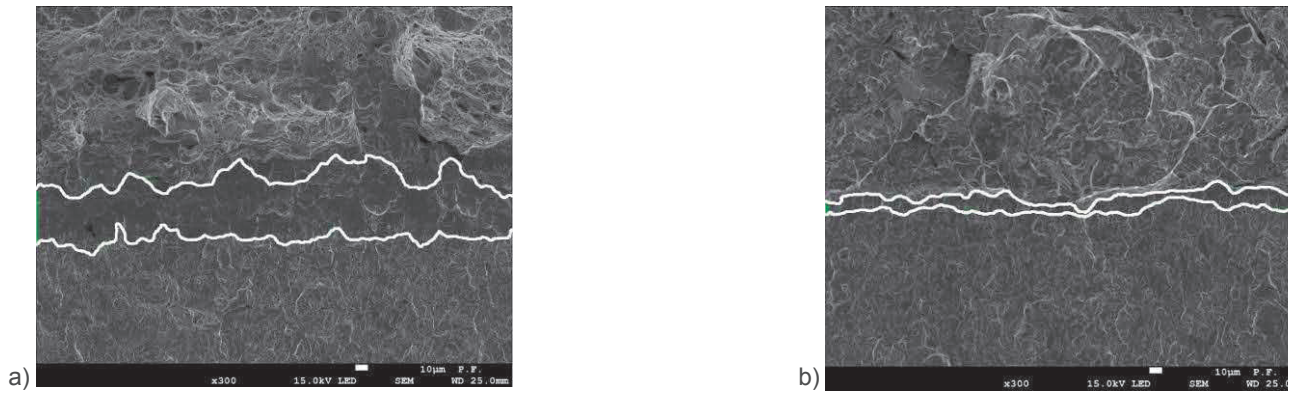

Figure 4 Example pictures of SEM with marked fields of the stretch zone surface for specimens for test temperature a) 20 ^{0}C, b) -80 ^{0}C

Table 2 Calculation results for T_z i d_n

T_{TEST}	+20 °C	-10 °C	-20 °C	-50 °C	-80°C
T_z	0.452	0.452	0.444	0.458	0.461
d_n	0.632	0.647	0.67	0.664	0.677
$\Delta\bar{a}_{SZW}$ [μm]	46.04	27.90	25.79	18.45	10.00
J_i [kN / m]	156.26	94.22	85.15	59.06	34.31
J^*_{IC} [kN / m]	246.73	130.86	107.47	57.67	35.51

The critical values of fracture toughness at the fracture initiation instant, J_i were computed using formula (1) on the basis of the mean value of the SZW, $\Delta\bar{a}_{SZW}$. **Table 2** shows, for appropriate temperatures, the results of calculations of coefficients T_Z and d_n, of the $\Delta\bar{a}_{SZW}$ and critical values, J_i. The critical values J^*_{IC}, which correspond to averaged values, found from the exponential regression, are also provided.

Figure 2a shows exemplary profiles of curves that illustrate the loading of SEN(B) specimens at different temperatures. As temperature is reduced, the dependence is broken earlier. That indicates fracture initiation occurs at a lower energy level that corresponding to lower values of integral J. In **Figure 5** the J_{IC} data are denoted as (x), and data J_i - (♦). When temperature reduced, the lower values of both J_{IC} and J_i were observed. Large scatter of data is characteristic for values of J_{IC}, especially in the temperature range (-20 ÷ 20 °C). Then, the subcritical crack growth proceeds due to the mixed mechanism, i.e. ductile and brittle one. The scatter is caused by large inclusion particles that are found in Hardox-400 steel. Although their percentage content is low, they can cause brittle fracture if they are located in front of the crack tip, where the maximum level of the opening stress is found [14]. As the temperature is lowered, the cleavage fracture becomes initiated by particles of smaller sizes, mainly particles of carbide precipitates. The percentage content of such particles is high, and it grows with a decrease in temperature that leads to reduced values J_{IC}, J_i and diminished data scatter band (**Figure 5**). The data were approximated with the exponential function which represents the dependence $J_{IC} = f(T)$ for averaged data.

Critical values of the integral J at the instant of subcritical fracture initiation, J_i, in the temperature range for which the subcritical fracture growth proceeds according to the mixed mechanism (-20 ÷ 20 °C), are located lower than J_{IC}. In **Figure 5**, values of J_i were computed for specimens that showed J_{IC} values close to the regression function curve. The difference increases with a rise of the experimental temperature. The reason why differences in J_{IC} and J_i values occur is the fact that for ductile growth of the subcritical crack, J_{IC} is characterised by fracture toughness for averaged growth having the length of Δa = 0.2 mm, while J_i - at the instant of initiation. For ductile growth, the energy necessary for subcritical crack to grow is taken into account when J_{IC} value is calculated. In cleavage cracking, however, when the crack propagation is carried out at the expense of the specimen elastic strain energy, the values J_{IC} and J_i that are obtained are close to each other.

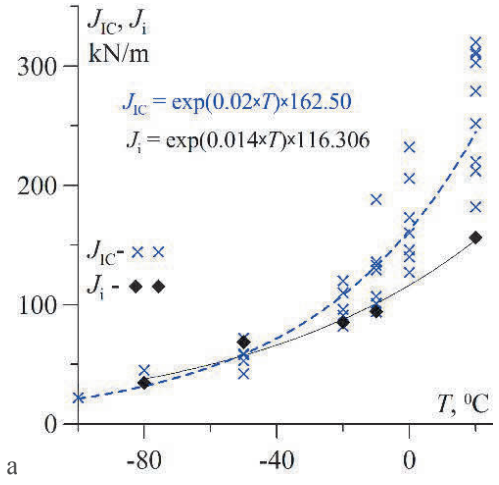

Figure 5 Critical values of J_{IC} (x) and J_i (♦) on test temperature

4. SUMMARY

The paper presented thorough investigations into strength properties and fracture toughness of high strength Hardox-400 steel. The investigations covered the temperature range of ductile-to-brittle transition mechanism. It was shown that large scatter of values of strength properties and fracture toughness characteristic of Hardox-

400 steel is caused by inhomogeneity of microstructure and occurrence of large inclusion particles like nitrides, sulphates and oxides. It was observed that the scatter bands decrease with temperature lowering. Similar trends with respect to temperature-dependent changes of the materials properties were obtained for high-strength ferritic S960QC steel [15]. The dependence of changes in strength characteristics and fracture toughness on temperature was presented in the form of a function. Changes in strength characteristics are well described by linear functions. The fracture toughness dependence was shown by means of the exponential function. Presenting materials properties in the form of a function makes it possible to obtain averaged values that account for the whole set of data. The data should be utilised in further strength analyses and numerical simulations.

ACKNOWLEDGEMENTS

The study was carried out within the framework of research projects financed by Poland's Ministry of Science and Higher Education 01.0.08.00/2.01.01.01.0008MNSP.MKPK.16.001; no. 01.0.06.00/2.01.01.02.0020 MNSC.MKTK.16004; no. 01.0.08.00/2.01.01.00.0049; MNSP.MKPK.15.001

REFERENCES

[1] DZIOBA, I., PAŁA, R., PAŁA, T. Temperature dependency of fracture toughness of high-strength Ferritic steel Hardox-400. Acta Mechanica Et Automatica, 2013, vol. 7, no. 4, pp. 125-129.

[2] DUDZIŃSKI, W., KONAT, Ł., PĘKALSKA, L., PĘKALSKI, G. Struktury i właściwości stali Hardox 400 i Hardox 500. Inżynieria Materiałowa, 2006, pp. 139-142.

[3] http://stalhardox.pl/images/pdf/151_HARDOX_400.pdf

[4] ASTM E1820-09. Standard Test Method for Measurement of Fracture Toughness, Annual book of ASTM standards. (2011).

[5] ASTM, E1737-96. Standard Test Method for J-integral Characterization of Fracture Toughness.

[6] ESIS Procedure for Determining the Fracture Behaviour of Materials. ESIS P2-92 (1992). Appendix 4. s.A4.1-A4.6.

[7] SCHWALBE, K. H., LANDES, J.D., HEERENS, J. Classical Fracture Mechanics Methods. GKSS 2007/14.2007.

[8] ISO 12135:2002 Metallic materials - Unified method of test for the determination of quasistatic fracture toughness.

[9] MIYAMOTO, H., KOBAYASHI, H., OHTSUKA, N. Elastic-Plastic Fracture Toughness JIC . Test Method Recommended in Japan, 1985, pp. 550-558.

[10] NEIMITZ A. Mechanika Pękania. 1st ed. Warszawa: PWN. 1999, 25 p.

[11] GUO, W. Elasto-Plastic Three-Dimensional Crack Border Field - III. Fracture Parameters. Engineering Fracture Mechanics, 1995, vol. 51, no. 1, pp. 51-71.

[12] KOBAYASHI, H., NAKAMURA, H., NAKAZAWA, H. Evaluation of Blunting Line and Elastic-Plastic Fracture Toughness. ASTM STP 803, 1983: pp.420-438.

[13] https://imagej.nih.gov/ij/

[14] DZIOBA, I., GAJEWSKI, M., NEIMITZ, A. Studies of fracture processes in Cr-Mo-V ferritic steel with various types of microstructure. International Journal of Pressure Vessels and Piping, 2010, vol. 87, no. 10, pp. 575-586.

[15] NEIMITZ, A., DZIOBA, I., LIMNELL, T. Master Curve of ultra-high strength steel. International Journal of Pressure Vessels and Piping, 2012, vol. 92, pp. 19-26.